Published in final edited form as:
Ann Biomed Eng. 2009 October ; 37(10): 1922–1933. doi:10.1007/s10439-009-9643-z.

Perfluorocarbon Nanoemulsions for Quantitative Molecular Imaging and Targeted Therapeutics

Megan M. Kaneda[1,2], **Shelton Caruthers**[1,2,3], **Gregory M. Lanza**[2,4], and **Samuel A. Wickline**[2,4]

[1]Department of Biomedical Engineering, Washington University, St Louis, MO, USA

[2]Consortium for Translational Research in Advanced Imaging and Nanomedicine, Campus Box 8215, 4444 Forest Park Avenue, St Louis, MO 63108, USA

[3]Philips Healthcare, Andover, MA, USA

[4]Department of Medicine, Washington University, St Louis, MO, USA

Abstract

A broad array of nanomaterials is available for use as contrast agents for molecular imaging and drug delivery. Due to the lack of endogenous background signal *in vivo* and the high NMR sensitivity of the ^{19}F atom, liquid perfluorocarbon nanoemulsions make ideal agents for cellular and magnetic resonance molecular imaging. The perfluorocarbon core material is surrounded by a lipid monolayer which can be functionalized with a variety of agents including targeting ligands, imaging agents and drugs either individually or in combination. Multiple copies of targeting ligands (~20–40 monoclonal antibodies or 200–400 small molecule ligands) serve to enhance avidity through multivalent interactions while the composition of the particle's perfluorocarbon core results in high local concentrations of ^{19}F. Additionally, lipophilic drugs contained within molecularly targeted nanoemulsions can result in contact facilitated drug delivery to target cells. Ultimately, the dual use of perfluorocarbon nanoparticles for both site targeted drug delivery and molecular imaging may provide both imaging of disease states as well as conclusive evidence that drug delivery is localized to the area of interest. This review will focus on liquid perfluorocarbon nanoparticles as ^{19}F molecular imaging agents and for targeted drug delivery in cancer and cardiovascular disease.

Keywords

Fluorine; Molecular imaging; Perfluorocarbon; Targeted drug delivery; Nanoparticles

INTRODUCTION

Perfluorocarbons (PFCs) are synthetic organic compounds in which all or most of the hydrogen atoms have been replaced with fluorine atoms. These molecules have the unique property of being both lipophobic and hydrophobic. The use of perfluorocarbons has been explored for various medical applications, including percutaneous transluminal cardiac angioplasty (PTCA),[7,20] partial liquid lung ventilation,[8,17,24] gastrointestinal X-ray contrast agent,[3,54] and

Address correspondence to Samuel A. Wickline, Consortium for Translational Research in Advanced Imaging and Nanomedicine, Campus Box 8215, 4444 Forest Park Avenue, St Louis, MO 63108, USA. Electronic mail: saw@howdy.wustl.edu, saw@wuphys.wustl.edu.

blood substitutes.[6,14,22,31,42] As an example, Fluosol® from Green Cross was approved for intravascular use in the United States, and contains perfluorodecalin.

The tissue clearance time for perfluorocarbons varies based on the chemical compound. These tissue half-lives ranges from 4 days for perfluorooctylbromide (PFOB) to 65 days for perfluorotripropylamine. Clearance of these fluorocarbons takes place not through metabolism, but through slow dissolution back into the circulation by lipid carriers. Ultimately perfluorocarbons are eliminated through expiration.[37,43,56]

The design of targeted nanoscale molecular imaging agents must accomplish a long circulating half-life, sensitive and selective binding to the epitope of interest, prominent contrast-to-noise enhancement, acceptable toxicity, ease of clinical use, and ideally would be applicable with standard commercially available imaging systems. The use of nanoparticles or targeted nanoemulsions as carriers has the additional advantage of selectively delivering large payloads of imaging or therapeutic agents to the site of interest. Nanoscale micelles and surfactant-stabilized nanodroplets of PFCs can be created by self-assembly of molecules to produce agents that can be used for clinical cellular and molecular imaging.[6,50,51] NMR utilizing the unique signature from ^{19}F has been widely exploited for both spectroscopic studies and increasingly for magnetic resonance imaging (MRI). The ^{19}F atom exhibits high NMR sensitivity, with essentially no background signal within the body. This review will focus on the use of self-assembling liquid PFC nanoparticles for ^{19}F magnetic resonance molecular imaging and spectroscopy (MRS) and drug delivery in cancer and cardiovascular disease.

^{19}F NMR AND MOLECULAR MRI

The liquid perfluorocarbon core material in PFC nanoemulsions is surrounded by a lipid monolayer that can be functionalized to contain various agents for imaging or therapeutic action. Different core perfluorocarbons can be used, including perfluorodichlorooctane, perfluorodecalin, perfluoro 15-crown-5 ether (CE), and most commonly, perfluorooctyl bromide (PFOB). Multifunctional activity can be realized by incorporating combinations of one or more targeting ligands, imaging agents, and/or drugs into the formulation simultaneously. Materials can be covalently or noncovalently linked to the particle surface, dissolved in the coating (e.g., lipophilic drugs deposited in lipid membrane layers), or carried in the particle interiors for cellular deposition and activation (Fig. 1).

Multiple copies of binding ligands can be incorporated depending on the size of the particle. This serves to enhance avidity and target detectability by reducing the particle dissociation rate thus better securing the agent at the intended site. Typically, 20–40 monoclonal antibodies or 200–400 small molecule ligands can be attached to the surface of the particle.[26,28] Specificity is conferred by the targeting ligand itself, with dissociation constants generally in the nanomolar range, although high avidity agents may in part overcome this limitation through multivalent interactions.

Once the particle binding takes place, high avidity is conferred through multivalent interactions between the particle and cell surface. Particles that do not bind are conveniently removed by the liver and spleen. The particle size of the emulsion predicts both the vascular half-life and biodistribution. Pharmacokinetic analysis indicates a clearance half-life of approximately 3–6 h depending on species.[18] The tissue distribution reflects the expected activity of the macrophage phagocytic system where the spleen and the liver remove the majority of the particles after intravenous injection.[18] Ultimately, the optimal particle size of the emulsion should result in a vascular persistence that is clinically efficacious while limiting deep-tissue retention, which for most intravenous applications is approximately 200–400 nm.

The comparatively modest MRI contrast enhancement achievable with targeted contrast agents for molecular imaging necessitates the delivery of higher payloads of contrast materials, which can be provided by novel nanotechnologies. For PFC particles, the opportunity to employ a unique MRI/MRS signature emanating from its fluorine (^{19}F) core can be advantageous. [34] Recently, quantitative approaches have been described for molecularly targeted emulsions that allow the computation of concentration of bound nanoparticles under certain circumstances, based on either the ^{1}H or ^{19}F signals.[33,34]

NMR is a particularly rich phenomenon providing information through multiple parameters including chemical shift, relaxation processes (R_1 and R_2), scalar coupling, and chemical exchange, and each of these parameters has been exploited for speciflc ^{19}F NMR reporter molecules. The simplest concept of NMR is that of chemical shift and ^{19}F is exceptionally sensitive to molecular and micro environmental changes. Fluorine NMR has a very large chemical shift range (~300 ppm) allowing multiple agents to be examined simultaneously with minimal danger of signal overlap. NMR signal can be quantitative, so that the integral of a signal is directly proportional to the amount of material being interrogated. Detection sensitivity is governed by numerous parameters including the volume of interrogation, the required spatial resolution, and relaxation properties of the molecule and its tendency to accumulate or disperse from a region of interest.

The signal generated by the fluorine atoms within the perfluorocarbon core of PFC-based nanoparticles has been introduced as a unique signature for MR molecular imaging.[5,27,33,34,38] While not all nuclei exhibit the magnetic resonance effect and therefore cannot be measured directly, ^{19}F, like ^{1}H, has one unpaired proton and no unpaired neutrons, and thus with a net spin of ½, exhibits the NMR phenomenon. Serendipitously, the gyromagnetic ratio (γ) for ^{19}F is also close to that of ^{1}H(i.e., 40.1 vs. 42.6 MHz/T, respectively) which means that their resonance frequencies are relatively similar. Their relative signal strengths are also similar, with that of ^{19}F being approximately 83% that of ^{1}H. The liquid perfluorocarbon core represents 98% of the total nanoparticle volume, leading to a substantial ^{19}F concentration (~100 M) within typical perfluorooctylbromide particles.

While the ^{19}F isotope of fluorine has a natural abundance of near 100%, the biological presence is virtually zero. Therefore, the ^{19}F nuclei which are highly concentrated within the perfluorocarbon core of the nanoparticle emulsions are a prime candidate for direct MR spectroscopy and imaging without surrounding signal from endogenous fluorine (Fig. 2). This recent approach has been demonstrated for molecular imaging and spectroscopy of fibrin at 4.7 T and for quantifying the concentration of nanoparticle binding to a selected site based on localized fluorine spectroscopy and subsequently for stem cell imaging *in vivo*.[33,34,40]

Another use for ^{19}F imaging and spectroscopy of perfluorocarbon particles is in recognizing different targeted moieties on the same sample. Due to differences in their local nuclear environments (e.g., electron shielding, J-coupling, etc), different fluorine atoms resonate at slightly different frequencies so that they are often readily separable on an NMR spectrum.

This means that by using PFC nanoparticles formulated with different perfluorocarbon species, it is possible to target them to the same sample and quantify their presence separately with one spectroscopic scan as shown by Morawski *et al.*[34] in Fig. 3 for PFOB and crown ether compounds formulated as nanoemulsions. The ^{19}F signal was measured at 4.7 T from fibrin-targeted, paramagnetic perfluorocarbon nanoparticles by Morawski *et al.* to spectroscopically quantify the varying amounts of PFC nanoparticles bound to thrombi *in vitro*. The estimates of ^{19}F concentration based on MRS of ^{19}F matched the actual measured concentrations of particles. While spectroscopy will ultimately be most useful for quantification, other techniques allow imaging of the different perfluorocarbon particles as well. These may include frequency

selective excitation so that only the perfluorocarbon species of interest produces a signal or other forms of chemical shift imaging that have been developed for differentiating fat from water in clinical imaging.[5]

Applications

As an alternative to MR signal modeling or measuring the indirect effects of contrast agents on water molecules (e.g., T1 or T2 for ^{1}H), one could measure the ^{19}F signal of the contrast agent directly, as is the case for nuclear medicine radioisotopes. Given their high fluorine content, fibrin-targeted nanoparticles may provide quantification of exposed fibrin, indicating the size and/or number of ruptures in the fibrous cap. This technique was applied to human carotid endarterectomy samples to provide a quantitative measure of microscopic amounts of fibrin associated with ruptured atherosclerotic plaques in patients with carotid artery disease[34] (Fig. 4).

Imaging human carotid endarterectomy samples at 4.7 T, multi-slice ^{1}H MRI showed high levels of signal enhancement along the luminal surface due to binding of targeted paramagnetic nanoparticles to fibrin deposits. A ^{19}F projection image of the artery, acquired in less than 5 min, shows the asymmetric distribution of fibrin-targeted nanoparticles around the vessel wall corroborating the ^{1}H signal enhancement (Fig. 4). Spectroscopic quantification of nanoparticle binding allowed calibration of the ^{19}F MRI signal intensity. Co-registration of the quantitative nanoparticle map with the ^{1}H image permits visualization of anatomical and pathological information in a single image. Combining information from ^{1}H and ^{19}F MRI could allow prediction of subsequent occlusion or distal embolization from unstable or disrupted plaques, and aid clinical decision-making and triage to acute invasive intervention vs. pharmaceutical therapies.

Extending this paradigm to a 1.5 T MR system using rapid steady-state imaging techniques, *in vitro* fibrin-bound nanoparticles of two different species of perfluorocarbon (PFOB and CE) in varying volumes were not only quantified via clinically relevant imaging techniques, but were also identified and independently imaged based on their unique MR spectral signatures.[5] Both imaging and spectroscopy could distinguish nanoparticles containing either perfluorooctylbromide (PFOB) or perfluoro-15-crown-5-ether (CE) as the core material. The signal to noise for PFOB was lower than CE (10 vs. 25, respectively), presumably due to the single CE peak (20 equivalent fluorine atoms) compared to the multiple PFOB peaks (17 fluorine atoms distributed over 5 peaks). A clear linear relationship between the ^{19}F signal intensity and perfluorocarbon concentration was demonstrated for both PFOB and CE using both imaging and spectroscopy. From this demonstration on fibrin clots, one might extrapolate the potential of using multiple perfluorocarbon nanoparticle agents, each targeted to a different epitope, to perform noninvasive, “imaging-based immunohistochemistry”, e.g., quantifying simultaneously the amount of angiogenesis and exposed fibrin associated with an atherosclerotic plaque as an indicator of its pathophysiological significance.

The possibility for performing MR angiography with untargeted ^{19}F PFC nanoparticles has been explored by Morawski–Neubauer *et al.*[38] Because these agents are sized so as to remain in the vascular space, they might be used to define vessel geometry. This requires sufficient signal sensitivity, which depends in part on blood levels of fluorine. Using a rapid scanning technique (steady state free precession, SSFP) and custom designed coils, high level vascular signals were obtained at 1.5 T for *in vitro* and *ex vivo* samples. Also, *in vivo* imaging of rabbit carotid arteries was successful both during direct intra-arterial injection of agents and after noninvasive intravenous dosing and imaging under steady state conditions. This study represents the first demonstration of small vessel imaging at clinical field strengths with sufficient temporal resolution to view both first pass contrast enhancement and steady-state blood signals for nanoparticles delivered noninvasively at moderate doses. This dosage

corresponds to 1.5–2.5 mL emulsion per kg body weight (or, equivalently, 0.5–0.9 g perfluorocarbon per kg) and is well within the “absolute no effect dose” of 2.7–9 g PFC/kg determined using other PFC blood substitute emulsions. [14]

In addition to molecular imaging of fibrin and MR angiography, ^{19}F MRI has been used to track *dendritic cells* and endothelial precursor cells labeled with PFC nanoparticles.[2,40] Stem cell tracking by MRI has typically relied on iron oxide[1,4,23,55] or gadolinium agents,[19,32] but definitive identification of labeled cells can be difficult due to innate susceptibility artifacts and variations in ^{1}H signal intensity within the body.

Ahrens *et al.*[2] recently utilized fluorine nanoparticle MR molecular imaging approaches by employing a CE perfluorocarbon preparation of nanoparticles to load dendritic immune cells with no loss of viability. The expression of cell surface markers, including CD80 and MHC, was also not affected. Accordingly, they demonstrated an extension of the use of fluorine imaging at research field strengths (11.7 T) to track cells after local and systemic injections. The advantage to this approach is that no tissue background signal exists because there is no appreciable amount of fluorine in the body to confound the signal from the targeted cells.

Partlow *et al.*[40] reported methods for labeling of proangiogenic endothelial precursor cells with multiple types of perfluorocarbon nanoparticles for rapid imaging and spectroscopy at clinical (1.5 T) and research (11.7 T) field strengths (Fig. 5). These cells avidly ingest the PFC nanoparticles without the need for conjunctive transfection agents, such as lipofectamine, with no untoward effect on cell viability and preserved ability to contribute to cancer angiogenesis. This is likely due to the specific nature of the soft deformable particles and their interaction with the endothelial progenitor cells. Perfluorocarbon labeling of endothelial progenitor cells can be detected with ^{19}F spectroscopy on the order of days out to one week depending on the perfluorocarbon used. Moreover, not only can these cells be uniquely identified and tracked with MRI, but their local concentration can be quantified based on the ^{19}F spectral signature.

The capacity of targeted PFC nanoparticles to serve as a universal carrier of imaging agents can be extended to proton T_1-weighted MR imaging as well as nuclear and optical imaging. Because molecular epitopes of interest may reside on or inside of cells in very sparse quantities at low nanomolar or picomolar concentrations, considerable amplification of the local contrast effect might be achieved by incorporating large amounts of paramagnetic or other relaxing agents as the payload.[33] In the case of T^1-weighted imaging, the surface of the particle can be decorated with numerous copies of gadolinium chelates (100,000+) to achieve the micromolar concentrations required per voxel.[13] Paramagnetic PFC-based nanoparticles have been shown to yield substantial amplification of signal from fibrin clots at 1.5 T both *in vitro* and *in vivo*.[13,25,57] In the case of the experimental canine model used by Flacke *et al.*[13] *in vivo* contrast-to-noise ratios between clot and blood exceeding 100 were achieved. For nuclear imaging, the utility of ^{111}In-labeled $\alpha_v\beta_3$-integrin targeted PFC nanoparticles for the detection of angiogenesis has been demonstrated in the rabbit Vx-2 tumor model.[18] ^{111}In-labeled $\alpha_v\beta_3$-integrin targeted PFC nanoparticles yielded high tumor-to-muscle ratio signals, which was enhanced for the formulations with 10 nuclides per particle vs. one. The ^{111}In-labeled nanoparticles provided a high sensitivity, low-resolution signal from the tumor neovasculature that was easily recognized within 15–30 min after injection and which persisted for hours. Optical detection and *ex vivo* visualization has been shown with the complexation of fluorescent agents to the PFC nanoparticles. These nanoparticles can generate signals detectable by immunohistochemistry.[9,41] These applications demonstrate the capability of this system to produce diverse functionalizations of PFC nanoparticles for molecular imaging using various modalities.

DRUG DELIVERY

The potential dual use of nanoparticles for both imaging and site targeted delivery of therapeutic agents offers great promise for individualizing therapeutics. Image-based therapeutics with site-selective agents could enable conclusive assurance that the drug is reaching the intended target. In the case of particulate agents however, the mechanisms of drug delivery become more complicated such that serum concentrations are not necessarily indicative of the amount drug accessible to the desired site. Furthermore, targeting the carrier to the tissue of interest, the drug release is also localized to that area, resulting in a much higher effective drug concentration at the site than indicated by serum levels alone. The ability to quantify the local concentrations of these particles could be of great benefit for estimating local drug concentrations and developing new pharmacokinetic and pharmacodynamic paradigms to describe this new class of agents.

Mechanism of Nanoparticle Cell Interaction

The unique mechanism of drug delivery for highly lipophilic agents such as paclitaxel contained within perfluorocarbon emulsions depends on the close apposition between the nanoparticle carrier and the targeted cell membrane, and has been described as contact facilitated drug delivery.[27] In contrast liposomal drug delivery that typically requires endocytosis of entire particles followed by an endosomal release step to liberate the active compounds, the mechanism of drug transport for the PFC particles involves particle binding followed by lipid mixing the phospholipid surface components between the emulsion vesicle and the targeted cell membrane[9] (Fig. 6). This mechanism depends in part on the extent and frequency of contact between two lipid surfaces and the ability to form a hemifusion complex between the vesicle and the cell lipid layers to achieve the lipid mixing. Drugs, especially hydrophobic moieties contained in the lipid monolayer of the nanoparticle, then diffuse out into the cell lipid membrane along with other components (e.g., peptides, genes) of the nanoparticle lipid membrane.[45] Ultimately they are transported to the cytoplasm directly by energy requiring processes that involve lipid raft-dependent internalization but not the internalization of intact particles.[41] This eliminates the requirement of endosomal escape for drug activity.

The rate of lipid exchange and drug delivery can be greatly increased by the application of clinically safe levels of ultrasound energy that increase the propensity for hemifusion or enhance contact between the nanoparticles and the targeted cell membrane[9] (Fig. 7). Previously, disruptive ultrasonic methods have been applied to micrometer-sized bubbles to perforate cell membranes by concussive or streaming forces in the hope of enhancing local delivery of drugs, genes and other therapeutic agents through “temporary” membrane pores.[11,16,47,49] In contrast, Crowder *et al.*[9] first reported that noncavitational ultrasound energy can markedly augment delivery of lipophilic substances to selected cell types after molecular targeting, which neither produces nor requires disruption of cell membrane integrity.[9,44] Ultrasound (mechanical index $\propto$ 1.9) applied with a clinical ultrasound imaging system to nanoparticles targeted to $\alpha_v\beta_3$ integrins on C32 melanoma cancer cells *in vitro* produced no untoward effects. With ultrasound exposure of 5 min, lipid delivery from the nanoparticles into the cytoplasm of C32 melanoma cells was dramatically augmented. This approach should allow focused delivery of sufficient energy to deep tissue to activate drug deposition from molecularly targeted nanoparticle carriers, while avoiding any potentially harmful bioeffects of the ultrasound *per se* to the targeted or other surrounding cells.

The physical mechanisms responsible for this phenomenon entail the action of quantifiable “radiation forces” on particles that are induced by the traveling compressional (ultrasound) waves,[10,48] which can increase biophysical interactions of nanoparticles with the targeted cell surface. Recent studies by Soman *et al.*[46] extend this concept to the delivery of bulky

therapeutic cargo (nanogold DPPE) with nanoparticles targeted $\alpha_v\beta_3$ integrins. In these studies, non-cavitational ultrasound used in conjuction with PFC-nanoparticles produced the uptake and delivery of lipids to the cytosol that would otherwise remain on the cell surface. These methods offer additional mechanisms for facilitating targeted drug delivery with the application of exogenous, safe ultrasound energy in conjunction with therapeutic targeted nanoparticles. The success of such "double targeting" strategies ultimately may allow the use of even lower systemic doses of highly effective agents.

Therapeutic Applications of Targeted Perfluorocarbon Nanoparticles

The contact facilitated mechanism of targeted drug delivery with the perfluorocarbon nanoparticles was first demonstrated *in vitro* with PFC particles targeted to smooth muscle cells (via tissue factor) delivering antiproliferative therapy (doxorubicin or paclitaxel). These studies indicated a potent antiproliferative effect for paclitaxel regardless of drug loading dose (0.2 or 2.0 mol.%).[27] When untargeted, the paclitaxel-laden nanoparticles exerted no effect on cell proliferation, indicating the requirement for a nanoparticle binding event for efficient drug delivery. Similar observations were made for doxorubicin, although due to its greater water solubility as compared with paclitaxel, some antiproliferative effect was also noted even without selective cell targeting. These initial proof of concept experiments have led to the development of targeted therapeutics using this platform for cardiovascular disease and cancer.

In Vivo Targeted Anti-angiogenic Therapy for Atherosclerosis

Angiogenesis of the *vasa vasorum* is required for the progression of atherosclerosis and perhaps for the production of unstable plaque.[21,30,35,39] Plaque neovasculature serves as both a biomarker of early disease, a harbinger of vulnerable plaque, and a useful entry point for therapeutic delivery. Moulton *et al.*[36] showed that anti-angiogenic therapy reduces the rate of plaque growth in the apolipoprotein E-insufficient mouse model of atherosclerosis. Administration of the anti-angiogenic drug TNP-470, a water-soluble analog of fumagillin derived as a natural product of *Aspergillus fumigatus* fungus, at 30 mg/kg every other day for 16 weeks inhibited the plaque growth by 70%.

Along these lines, Winter *et al.*[52] utilized the cholesterol-fed rabbit model of early atherosclerosis to determine the efficacy of anti-angiogenic therapy. Rabbits on a high cholesterol diet were treated with one of three emulsions: $\alpha_v\beta_3$-targeted fumagillin-loaded nanoparticles, $\alpha_v\beta_3$-targeted nanoparticles without fumagillin, and non-targeted fumagillin-loaded nanoparticles. All three nanoparticle types included gadolinium so that MRI could be performed at treatment to assess the level of plaque angiogenesis as indicated by molecular imaging of $\alpha_v\beta_3$-integrin expression, while simultaneously confirming and quantifying the specific binding of drug-laden nanoparticles, if targeted. One week later, all rabbits were re-imaged using diagnostic $\alpha_v\beta_3$-targeted paramagnetic nanoparticles to evaluate the response of the $\alpha_v\beta_3$-integrin, and hence the plaque neovasculature, to fumagillin therapy. The group that received the targeted anti-angiogenic nanoparticles exhibited a significant reduction in both the spatial distribution and level of $\alpha_v\beta_3$-related signal enhancement; whereas the groups which received no drug or non-targeted drug-carrying nanoparticles exhibited no therapeutic effect (Fig. 8). Histological analysis confirmed that neovasculature was concentrated in areas of the adventitia overlying regions of intimal thickening, and that neovasculature was significantly suppressed in those rabbits treated with $\alpha_v\beta_3$-targeted anti-angiogenic nanoparticles. Furthermore, the T_1-weighted MR image signal enhancement on the day of initial treatment with the $\alpha_v\beta_3$-targeted anti-angiogenic paramagnetic nanoparticles predicted therapeutic responsiveness (or, reduced $\alpha_v\beta_3$-integrin signal) on one-week follow-up MR imaging.

Targeted Thrombolytic Therapy

Thrombolysis is a clinical mainstay for rapid intervention in patients with acute myocardial infarction and stroke. However, serious systemic side effects can arise in the form of bleeding, hemorrhagic stroke, allergic reactions, and excitotoxicity. Although a number of modifications to active thrombolytic agents have been considered and tested to in an attempt to reduce side effects of drugs, such as streptokinase or tissue plasminogen activator (tPA), tPA remains the dominant agent in clinical use.

Marsh *et al.*[29] recently developed fibrin-targeted nanoparticles whose surfaces were modified to incorporate streptokinase, a traditional bacterial-derived thrombolytic enzyme that acts to convert plasminogen into its active fibrinolytic form, plasmin. The streptokinase was covalently coupled to the PFC nanoparticles with the use of 1.0 mol.% 1,2-dipalmitoyl-sn glycero-3-phosphoethanolamine-*N*-4-(*p*-maleimidophenyl)butyramide (MPB-PE; Avanti Polar Lipids) for coupling *N*-succinimidyl-S-acetylthioacetate (SATA)-derivatized streptokinase. Fibrin thrombi *in vitro* were targeted with the nanoparticles and imaged with high frequency ultrasound to illustrate binding based on enhanced acoustic back-scatter from the clot surfaces, which permitted volumetric estimates. Profile backscatter plots of the detected clot surface demonstrated that streptokinase-loaded, fibrin-targeted nanoparticles in the presence of plasminogen induced rapid fibrinolysis in less than 60 min with nearly total loss of fibrin volume (Fig. 9). In contrast, streptokinase-loaded or control fibrin-targeted nanoparticles incubated with buffer alone (i.e., no plasminogen available for conversion to plasmin) had no effect on clot volume over the course of the study. Morphologic changes exhibited in the treated group were accompanied by temporal and spatial changes in backscatter from the targeted surfaces indicative of the local action of the thrombolytic agent. This new nanoparticle-based thrombolytic agent may prove suitable for rapid and safe administration and could decrease the time from the ischemic event to reperfusion and lessen the morbidity and mortality of stroke.

In Vivo Targeted Anti-angiogenic Therapy for Cancer

Anti-angiogenic agents for cancer have assumed a critical role in the therapeutic armamentarium for solid tumors subsequent to the demonstration of the efficacy of Avastin™ for various tumor types.[12,15] Although a number of agents have been tested clinically, either lack of efficacy or systemic toxicity has limited their clinical adoption. To develop an approach that might deliver far more agent locally to intended sites of tumor angiogenesis by cell-selective contact-facilitated mechanisms, while simultaneously requiring far less systemic drug levels, Winter *et al.*[53] have utilized the $\alpha_v\beta_3$-targeted fumagillin-loaded nanoparticles to suppress neovasculature and inhibit the growth of Vx-2 adenocarcinoma xenografts. Fumagillin, incorporated in minute doses into $\alpha_v\beta_3$-targeted nanoparticles result in a decrease in Vx-2 tumor volume and a decrease in neovascular area without reticuloendothelial clearance organ toxiticy or neurocognitive dysfunction. Therapeutic efficacy for these targeted compounds was demonstrated at systemic doses that are 1000-fold lower than previous animal studies and 60-fold lower than has been tested clinically for related anti-angiogenic compounds (TNP-470).

CONCLUSIONS

Targeted perfluorocarbon (^{19}F) nanoparticles and other small molecule agents can offer unique and potentially quantitative signatures for molecular MRI and MRS with no competing background signal. Additionally, these perfluorocarbon nanoemulsions can be used to deliver lipophilic therapeutic agents in a site specific manner through contact mediated drug delivery while concurrently serving as direct confirmation of delivery via ^{19}F MRI/MRS. Multimodal imaging can be performed simultaneously, and multi-spectral detection with the use of different

perfluorocarbons is possible. Sensitive image and spectral signal detection will benefit from improvements in both hardware and software as this nascent application moves into the clinical evaluation phase.

ACKNOWLEDGMENTS

This work was supported by the American Heart Association (0810144Z to MMK), the National Institutes of Health (HL073646 and CA119342 to SAW) and Philips Healthcare. SAW and GML are cofounders, equity holders and board members of Kereos, Inc. SDC is employed by Philips Healthcare.

REFERENCES

1. Ahrens ET, Feili-Hariri M, Xu H, Genove G, Morel PA. Receptor-mediated endocytosis of iron-oxide particles provides efficient labeling of dendritic cells for in vivo mr imaging. Magn. Reson. Med 2003;49:1006–1013. [PubMed: 12768577]doi:10.1002/mrm.10465
2. Ahrens ET, Flores R, Xu H, Morel PA. In vivo imaging platform for tracking immunotherapeutic cells. Nat. Biotechnol 2005;23:983–987. [PubMed: 16041364]doi:10.1038/nbt1121
3. Brown JJ, Duncan JR, Heiken JP, Balfe DM, Corr AP, Mirowitz SA, Eilenberg SS, Lee JK. Perfluoroctylbromide as a gastrointestinal contrast agent for mr imaging: use with and without glucagon. Radiology 1991;181:455–460. [PubMed: 1924788]
4. Bulte JW, Kraitchman DL. Monitoring cell therapy using iron oxide mr contrast agents. Curr. Pharm. Biotechnol 2004;5:567–584. [PubMed: 15579045]doi:10.2174/1389201043376526
5. Caruthers SD, Neubauer AM, Hockett FD, Lamerichs R, Winter PM, Scott MJ, Gaffney PJ, Wickline SA, Lanza GM. In vitro demonstration using 19f magnetic resonance to augment molecular imaging with paramagnetic perfluorocarbon nanoparticles at 1.5 tesla. Invest. Radiol 2006;41:305–312. [PubMed: 16481914]doi:10.1097/01.rli.0000199281.60135.6a
6. Clark LC Jr, Clark EW, Moore RE, Kinnett DG, Inscho EI Jr. Room temperature-stable biocompatible fluorocarbon emulsions. Prog. Clin. Biol. Res 1983;122:169–180. [PubMed: 6878358]
7. Cowley MJ, Snow FR, DiSciascio G, Kelly K, Guard C, Nixon JV. Perfluorochemical perfusion during coronary angioplasty in unstable and high-risk patients. Circulation 1990;81:IV27–IV34. [PubMed: 2306847]
8. Croce MA, Fabian TC, Patton JH Jr, Melton SM, Moore M, Trenthem LL. Partial liquid ventilation decreases the inflammatory response in the alveolar environment of trauma patients. J. Trauma 1998;45:273–280. [PubMed: 9715184]discussion 280-272
9. Crowder KC, Hughes MS, Marsh JN, Barbieri AM, Fuhrhop RW, Lanza GM, Wickline SA. Sonic activation of molecularly-targeted nanoparticles accelerates transmembrane lipid delivery to cancer cells through contact-mediated mechanisms: implications for enhanced local drug delivery. Ultrasound Med. Biol 2005;31:1693–1700. [PubMed: 16344131]doi:10.1016/j.ultrasmedbio.2005.07.022
10. Dayton P, Klibanov A, Brandenburger G, Ferrara K. Acoustic radiation force in vivo: a mechanism to assist targeting of microbubbles. Ultrasound Med. Biol 1999;25:1195–1201. [PubMed: 10576262] doi:10.1016/S0301-629(99)00062-9
11. Deng CX, Sieling F, Pan H, Cui J. Ultrasound-induced cell membrane porosity. Ultrasound Med. Biol 2004;30:519–526. [PubMed: 15121254]doi:10.1016/j.ultrasmedbio.2004.01.005
12. Ferrara N, Hillan KJ, Gerber HP, Novotny W. Discovery and development of bevacizumab, an anti-vegf antibody for treating cancer. Nat. Rev. Drug Discov 2004;3:391–400. [PubMed: 15136787]doi: 10.1038/nrd1381
13. Flacke S, Fischer S, Scott MJ, Fuhrhop RJ, Allen JS, McLean M, Winter P, Sicard GA, Gaffney PJ, Wickline SA, Lanza GM. Novel mri contrast agent for molecular imaging of fibrin: implications for detecting vulnerable plaques. Circulation 2001;104:1280–1285. [PubMed: 11551880]doi: 10.1161/hc3601.094303
14. Flaim SF. Pharmacokinetics and side effects of perfluorocarbon-based blood substitutes. Artif. Cells Blood Substit. Immobil. Biotechnol 1994;22:1043–1054. [PubMed: 7849908]doi: 10.3109/ 10731199409138801
15. Folkman J. Angiogenesis and apoptosis. Semin. Cancer Biol 2003;13:159–167. [PubMed: 12654259] doi:10.1016/S1044-579X(02)00133-5

16. Guzman HR, Nguyen DX, Khan S, Prausnitz MR. Ultrasound-mediated disruption of cell membranes. I. Quantification of molecular uptake and cell viability. J. Acoust. Soc. Am 2001;110:588–596. [PubMed: 11508983]doi:10.1121/1.1376131

17. Hirschl RB, Croce M, Gore D, Wiedemann H, Davis K, Zwischenberger J, Bartlett RH. Prospective, randomized, controlled pilot study of partial liquid ventilation in adult acute respiratory distress syndrome. Am. J. Respir. Crit. Care Med 2002;165:781–787. [PubMed: 11897644]

18. Hu G, Lijowski M, Zhang H, Partlow KC, Caruthers SD, Kiefer G, Gulyas G, Athey P, Scott MJ, Wickline SA, Lanza GM. Imaging of vx-2 rabbit tumors with alpha(nu)beta3-integrin-targeted 111in nanoparticles. Int. J. Cancer 2007;120:1951–1957. [PubMed: 17278104]doi:10.1002/ijc.22581

19. Jacobs RE, Fraser SE. Magnetic resonance microscopy of embryonic cell lineages and movements. Science 1994;263:681–684. [PubMed: 7508143]doi:10.1126/science.7508143

20. Jaffe CC, Wohlgelernter D, Cabin H, Bowman L, Deckelbaum L, Remetz M, Cleman M. Preservation of left ventricular ejection fraction during percutaneous transluminal coronary angioplasty by distal transcatheter coronary perfusion of oxygenated fluosol da 20%. Am. Heart J 1988;115:1156–1164. [PubMed: 2967624]doi:10.1016/0002-8703(88) 90002-6

21. Jain RK, Finn AV, Kolodgie FD, Gold HK, Virmani R. Antiangiogenic therapy for normalization of atherosclerotic plaque vasculature: a potential strategy for plaque stabilization. Nat. Clin. Pract. Cardiovasc. Med 2007;4:491–502. [PubMed: 17712362]doi:10.1038/ncpcardio0979

22. Keipert PE, Otto S, Flaim SF, Weers JG, Schutt EA, Pelura TJ, Klein DH, Yaksh TL. Influence of perflubron emulsion particle size on blood half-life and febrile response in rats. Artif. Cells Blood Substit. Immobil. Biotechnol 1994;22:1169–1174. [PubMed: 7849919]doi: 10.3109/ 10731199409138812

23. Kircher MF, Allport JR, Graves EE, Love V, Josephson L, Lichtman AH, Weissleder R. In vivo high resolution three-dimensional imaging of antigen-specific cytotoxic t-lymphocyte trafficking to tumors. Cancer Res 2003;63:6838–6846. [PubMed: 14583481]

24. Lane T. A. Perfluorochemical-based artificial oxygen carrying red cell substitutes. Transfus. Sci 1995;16:19–31. [PubMed: 10155703]doi:10.1016/0955-3886(94)00067-T

25. Lanza GM, Lorenz CH, Fischer SE, Scott MJ, Cacheris WP, Kaufmann RJ, Gaffney PJ, Wickline SA. Enhanced detection of thrombi with a novel fibrin-targeted magnetic resonance imaging agent. Acad. Radiol 1998;5:S173–S176. [PubMed: 9561074]discussion S183-174

26. Lanza GM, Wickline SA. Targeted ultrasonic contrast agents for molecular imaging and therapy. Prog. Cardiovasc. Dis 2001;44:13–31. [PubMed: 11533924]doi:10.1053/pcad.2001. 26440

27. Lanza GM, Yu X, Winter PM, Abendschein DR, Karukstis KK, Scott MJ, Chinen LK, Fuhrhop RW, Scherrer DE, Wickline SA. Targeted antiproliferative drug delivery to vascular smooth muscle cells with a magnetic resonance imaging nanoparticle contrast agent: implications for rational therapy of restenosis. Circulation 2002;106:2842–2847. [PubMed: 12451012]doi: 10.1161/01.CIR.0000044020.279 90.32

28. Lanza GM, Wickline SA. Targeted ultrasonic contrast agents for molecular imaging and therapy. Curr. Probl. Cardiol 2003;28:625–653. [PubMed: 14691443]doi:10.1016/j.cpcardiol.2003.11.001

29. Marsh JN, Senpan A, Hu G, Scott MJ, Gaffney PJ, Wickline SA, Lanza GM. Fibrin-targeted perfluorocarbon nanoparticles for targeted thrombolysis. Nanomedicine 2007;2:533–543. [PubMed: 17716136]doi:10.2217/17435889.2.4.533

30. McCarthy MJ, Loftus IM, Thompson MM, Jones L, London NJ, Bell PR, Naylor AR, Brindle NP. Angiogenesis and the atherosclerotic carotid plaque: an association between symptomatology and plaque morphology. J. Vasc. Surg 1999;30:261–268. [PubMed: 10436445]doi: 10.1016/S0741-5214(99)70136-9

31. McGoron AJ, Pratt R, Zhang J, Shiferaw Y, Thomas S, Millard R. Perfluorocarbon distribution to liver, lung and spleen of emulsions of perfluorotributylamine (ftba) in pigs and rats and perfluorooctyl bromide (pfob) in rats and dogs by 19f nmr spectroscopy. Artif. Cells Blood Substit. Immobil. Biotechnol 1994;22:1243–1250. [PubMed: 7849929]doi:10.3109/10731199409138822

32. Modo M, Mellodew K, Cash D, Fraser SE, Meade TJ, Price J, Williams SC. Mapping transplanted stem cell migration after a stroke: a serial, in vivo magnetic resonance imaging study. Neuroimage 2004;21:311–317. [PubMed: 14741669]doi:10.1016/j.neuroimage.2003.08.030

33. Morawski AM, Winter PM, Crowder KC, Caruthers SD, Fuhrhop RW, Scott MJ, Robertson JD, Abendschein DR, Lanza GM, Wickline SA. Targeted nanoparticles for quantitative imaging of sparse molecular epitopes with mri. Magn. Reson. Med 2004;51:480–486. [PubMed: 15004788]doi: 10.1002/mrm.20010
34. Morawski AM, Winter PM, Yu X, Fuhrhop RW, Scott MJ, Hockett F, Robertson JD, Gaffney PJ, Lanza GM, Wickline SA. Quantitative“Magnetic resonance immunohistochemistry” With ligand-targeted (19)f nanoparticles. Magn. Reson. Med 2004;52:1255–1262. [PubMed: 15562481]doi: 10.1002/mrm.20287
35. Moreno PR, Purushothaman KR, Sirol M, Levy AP, Fuster V. Neovascularization in human atherosclerosis. Circulation 2006;113:2245–2252. [PubMed: 16684874]doi: 10.1161/CIRCULATIONAHA.105.578955
36. Moulton KS, Heller E, Konerding MA, Flynn E, Palinski W, Folkman J. Angiogenesis inhibitors endostatin or tnp-470 reduce intimal neovascularization and plaque growth in apolipoprotein e-deficient mice. Circulation 1999;99:1726–1732. [PubMed: 10190883]
37. Naito R, Yokoyama K. An improved perfluorodecalin emulsion. Prog. Clin. Biol. Res 1978;19:81–89. [PubMed: 662887]
38. Neubauer AM, Caruthers SD, Hockett FD, Cyrus T, Robertson JD, Allen JS, Williams TD, Fuhrhop RW, Lanza GM, Wickline SA. Fluorine cardiovascular magnetic resonance angiography in vivo at 1.5 t with perfluorocarbon nanoparticle contrast agents. J. Cardiovasc. Magn. Reson 2007;9:565–573. [PubMed: 17365236]doi:10.1080/10976640600945481
39. O’Brien ER, Garvin MR, Dev R, Stewart DK, Hinohara T, Simpson JB, Schwartz SM. Angiogenesis in human coronary atherosclerotic plaques. Am. J. Pathol 1994;145:883–894. [PubMed: 7524331]
40. Partlow KC, Chen J, Brant JA, Neubauer AM, Meyerrose TE, Creer MH, Nolta JA, Caruthers SD, Lanza GM, Wickline SA. 19f magnetic resonance imaging for stem/progenitor cell tracking with multiple unique perfluorocarbon nanobeacons. Faseb J 2007;21:1647–1654. [PubMed: 17284484] doi:10.1096/fj.06-6505com
41. Partlow KC, Lanza GM, Wickline SA. Exploiting lipid raft transport with membrane targeted nanoparticles: a strategy for cytosolic drug delivery. Biomaterials 2008;29:3367–3375. [PubMed: 18485474]
42. Police AM, Waxman K, Tominaga G. Pulmonary complications after fluosol administration to patients with life-threatening blood loss. Crit. Care Med 1985;13:96–98. [PubMed: 3967511]doi: 10.1097/00003246-198502000-00008
43. Riess JG. The design and development of improved fluorocarbon-based products for use in medicine and biology. Artif. Cells Blood Substit. Immobil. Biotechnol 1994;22:215–234. [PubMed: 8087244] doi:10.3109/10731199409117416
44. Soman NR, Marsh JN, Hughes MS, Lanza GM, Wickline SA. Acoustic activation of targeted liquid perfluorocarbon nanoparticles does not compromise endothelial integrity. IEEE Trans. Nanobiosci 2006;5:69–75.doi:10.1109/TNB.2006.875052
45. Soman NR, Lanza GM, Heuser JM, Schlesinger PH, Wickline SA. Synthesis and characterization of stable fluorocarbon nanostructures as drug delivery vehicles for cytolytic peptides. Nano Lett 2008;8:1131–1136. [PubMed: 18302330]doi:10.1021/nl073290r
46. Soman NR, Marsh JN, Lanza GM, Wickline SA. New mechanisms for non-porative ultrasound stimulation of cargo delivery to cell cytosol with targeted perfluorocarbon nanoparticles. Nanotechnology 2008;19:185102–185109.doi:10.1088/0957-4484/19/18/185102
47. Taniyama Y, Tachibana K, Hiraoka K, Namba T, Yamasaki K, Hashiya N, Aoki M, Ogihara T, Yasufumi K, Morishita R. Local delivery of plasmid DNA into rat carotid artery using ultrasound. Circulation 2002;105:1233–1239. [PubMed: 11889019]doi:10.1161/hc1002.105228
48. ter Haar G, Wyard SJ. Blood cell banding in ultrasonic standing wave fields: a physical analysis. Ultrasound Med. Biol 1978;4:111–123. [PubMed: 734791]doi:10.1016/0301-5629(78)90036-4
49. Unger EC, McCreery TP, Sweitzer RH, Caldwell VE, Wu Y. Acoustically active lipospheres containing paclitaxel: a new therapeutic ultrasound contrast agent. Invest. Radiol 1998;33:886–892. [PubMed: 9851823]doi:10.1097/0000 4424-199812000-00007
50. Wickline SA, Lanza GM. Molecular imaging, targeted therapeutics, and nanoscience. J. Cell. Biochem. Suppl 2002;39:90–97. [PubMed: 12552608]doi:10.1002/jcb.10422

51. Wickline SA, Lanza GM. Nanotechnology for molecular imaging and targeted therapy. Circulation 2003;107:1092–1095. [PubMed: 12615782]doi:10.1161/01.CIR.0000059651.17045.77
52. Winter PM, Neubauer AM, Caruthers SD, Harris TD, Robertson JD, Williams TA, Schmieder AH, Hu G, Allen JS, Lacy EK, Zhang H, Wickline SA, Lanza GM. Endothelial alpha(v)beta3 integrin-targeted fumagillin nanoparticles inhibit angiogenesis in atherosclerosis. Arterioscler. Thromb. Vasc. Biol 2006;26:2103–2109. [PubMed: 16825592]doi:10.1161/01.ATV.0000235724.11299.76
53. Winter PM, Schmieder AH, Caruthers SD, Keene JL, Zhang H, Wickline SA, Lanza GM. Minute dosages of {alpha}{nu}{beta}3-targeted fumagillin nanoparticles impair vx-2 tumor angiogenesis and development in rabbits. Faseb J 2008;22:2758–2767. [PubMed: 18362202]
54. Wootton SL, Coley BD, Hilton SV, Edwards DK 3rd, Amberg JR, Mattrey RF. Value of brominated fluorocarbons for the radiographic diagnosis of small-bowel obstruction: comparison with other contrast agents in rats. AJR Am. J. Roentgenol 1993;161:409–416. [PubMed: 8333387]
55. Yeh TC, Zhang W, Ildstad ST, Ho C. Intracellular labeling of t-cells with superparamagnetic contrast agents. Magn. Reson. Med 1993;30:617–625. [PubMed: 8259062]doi:10.1002/mrm.1910300513
56. Yokoyama K, Yamanouchi K, Watanabe M, Matsumoto T, Murashima R, Daimoto T, Hamano T, Okamoto H, Suyama T, Watanabe R, Naito R. Preparation of perfiuorodecalin emulsion, an approach to the red cells substitute. Fed. Proc 1975;34:1478–1483. [PubMed: 1126445]
57. Yu X, Song SK, Chen J, Scott MJ, Fuhrhop RJ, Hall CS, Gaffney PJ, Wickline SA, Lanza GM. High-resolution mri characterization of human thrombus using a novel fibrin-targeted paramagnetic nanoparticle contrast agent. Magn. Reson. Med 2000;44:867–872. [PubMed: 11108623]doi: 10.1002/1522-2594(200012)44:6 <867::AID-MRM7> 3.0.CO;2-P

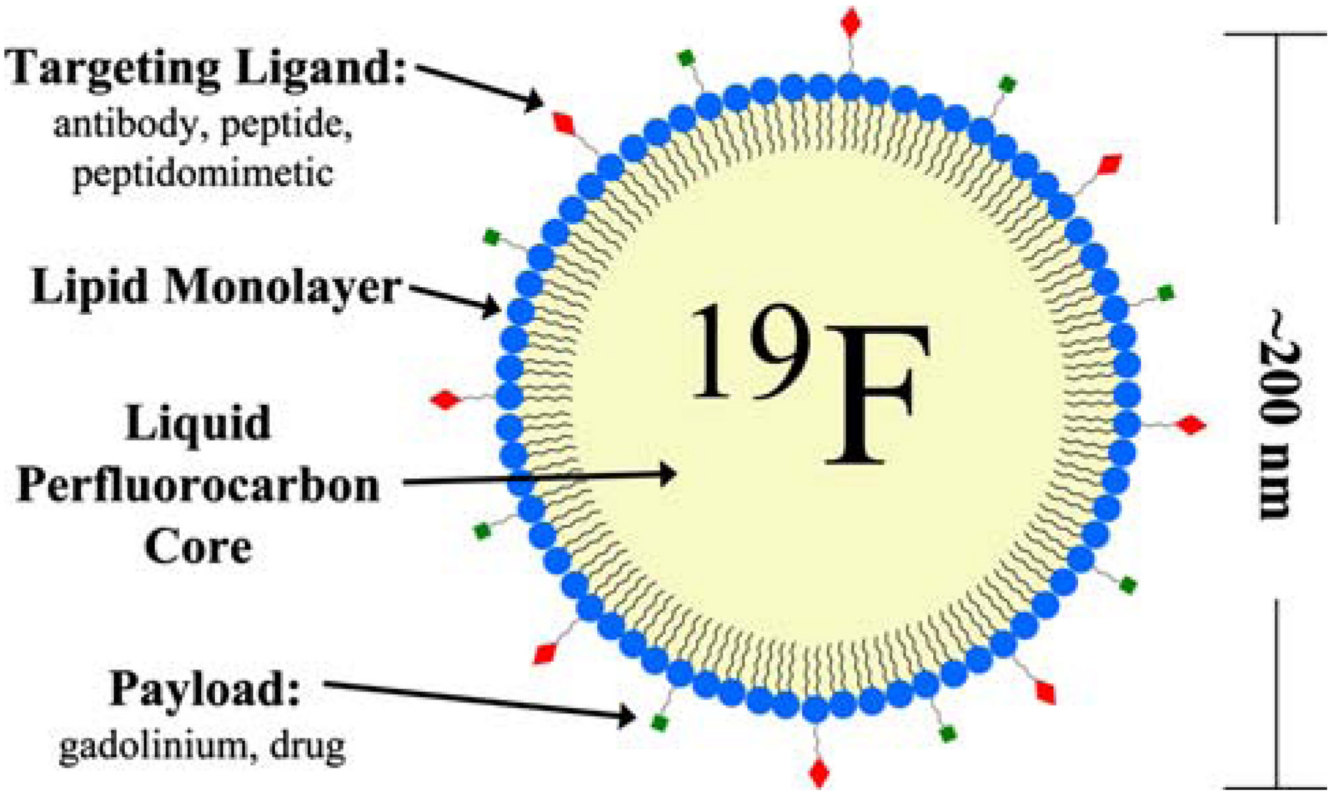

FIGURE 1.
A schematic representation of a multifunctional liquid perfluorocarbon nanoemulsion. The liquid perfluorocarbon core is surrounded by a lipid monolayer which can be functionalized with targeting ligands and other payload. Additionally, drugs can be dissolved in the lipid layer or carried in the particle interior.

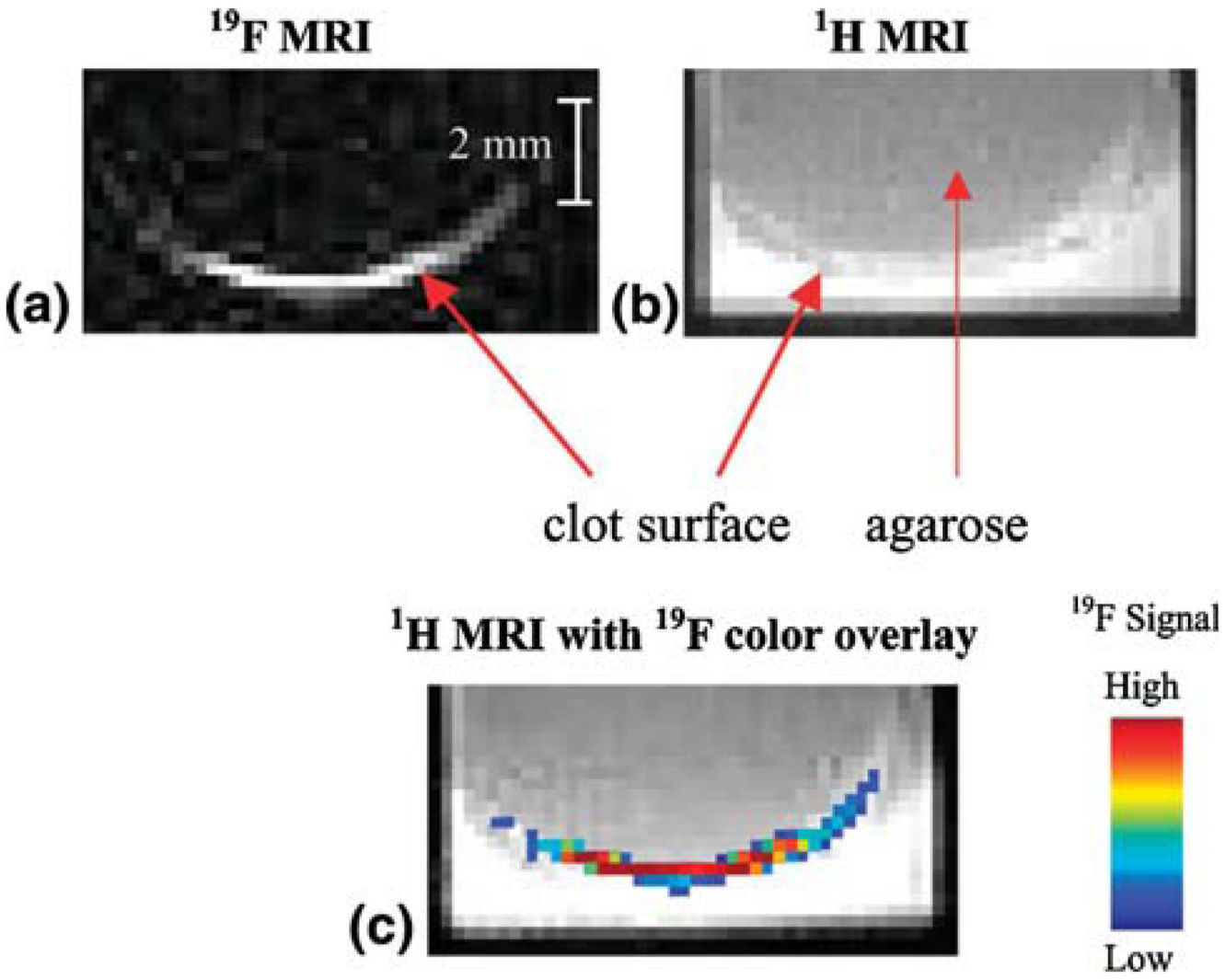

FIGURE 2.

(a) ^{19}F image (4.7 T) of a single slice through a clot *in vitro* treated with fibrin-targeted crown ether emulsion. High signal is observed at the clot surface due to bound fluorinated nanoparticles. (b) ^{1}H image (4.7 T) of the same slice showing the anatomy of the clot with significant background ^{1}H signal. (c) False color overlay of ^{19}F signal onto ^{1}H image clearly localizing ^{19}F signal to clot surface. (Reprinted with permission from Morawski *et al.*[34])

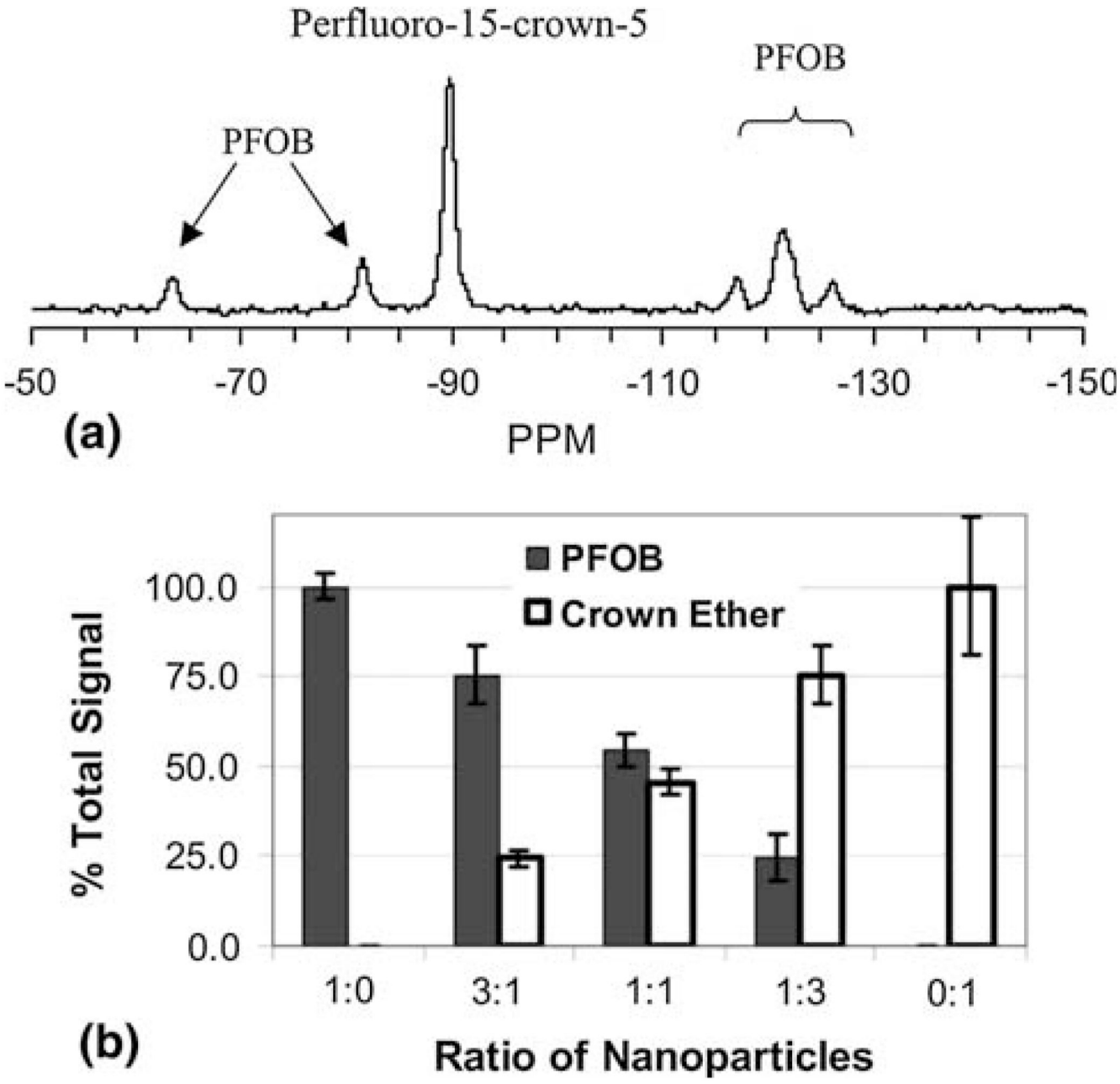

FIGURE 3.

(a) ^{19}F spectrum acquired at 4.7 T of a clot treated with a mixture of fibrin-targeted crown ether and PFOB emulsions. The crown ether peak and five discernible PFOB peaks are easily detected and individually resolved. (b) Percentage of total ^{19}F signal attributed to crown ether or PFOB for the clots treated with different nanoparticle mixtures, which are listed as the ratio of PFOB to crown ether. Spectral discrimination of crown ether and PFOB allows simultaneous quantification of the two nanoparticle species within a single sample. (Reprinted with permission from Morawski *et al.*[34])

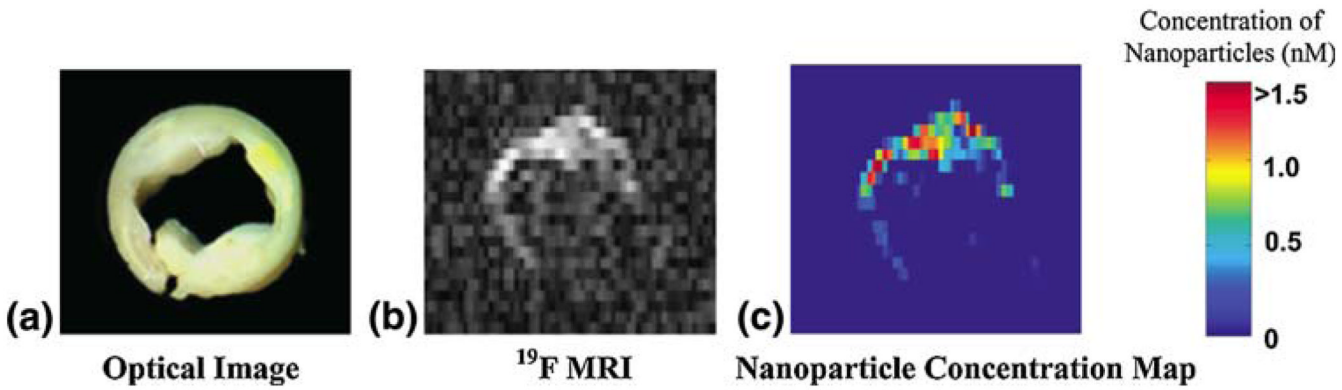

FIGURE 4.

(a) Optical image ex vivo of a 5-mm cross section of a human carotid endarterectomy sample. This section showed moderate luminal narrowing as well as several atherosclerotic lesions. (b) A ^{19}F projection image acquired at 4.7 T through the entire carotid artery sample shows high signal along the lumen due to nanoparticles bound to fibrin. (c) Concentration map of bound nanoparticles in the carotid sample. (Reprinted with permission from Morawski *et al.*[34])

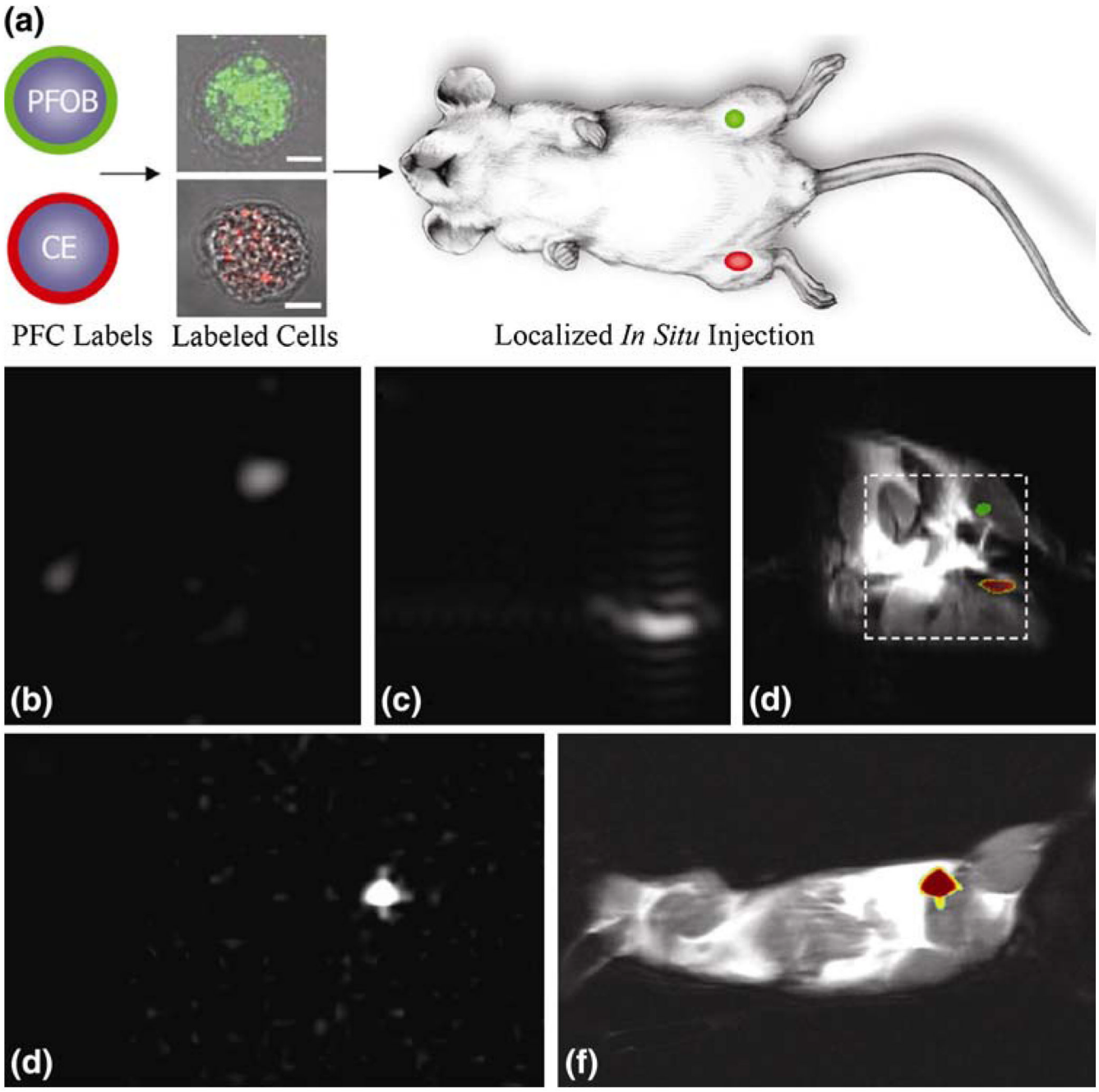

FIGURE 5.

Localization of labeled cells after *in situ* injection. (a) To determine the utility for cell tracking stem/progenitor cells labeled with either PFOB (green) or CE (red), nanoparticles were locally injected into mouse thigh skeletal muscle. (b–d) At 11.7 T, spectral discrimination permits imaging the fluorine signal attributable to ~1 × 106 PFOB-loaded (b) or CE-loaded cells (c) individually, which when overlaid onto a conventional ^{1}H image of the site (d) reveals PFOB and CE labeled cells localized to the left and right leg, respectively (dashed line indicates 3 × 3 cm^2 field of view for ^{19}F images). (e, f) Similarly, at 1.5 T, ^{19}F image of ~4 × 106 CE-loaded cells (e) locates to the mouse thigh in a ^{1}H image of the mouse cross section (f). The absence of background signal in ^{19}F images (b, c, e) enables unambiguous localization of

perfluorocarbon-containing cells at both 11.7 T and 1.5 T. (Reprinted with permission from Partlow *et al.*[40])

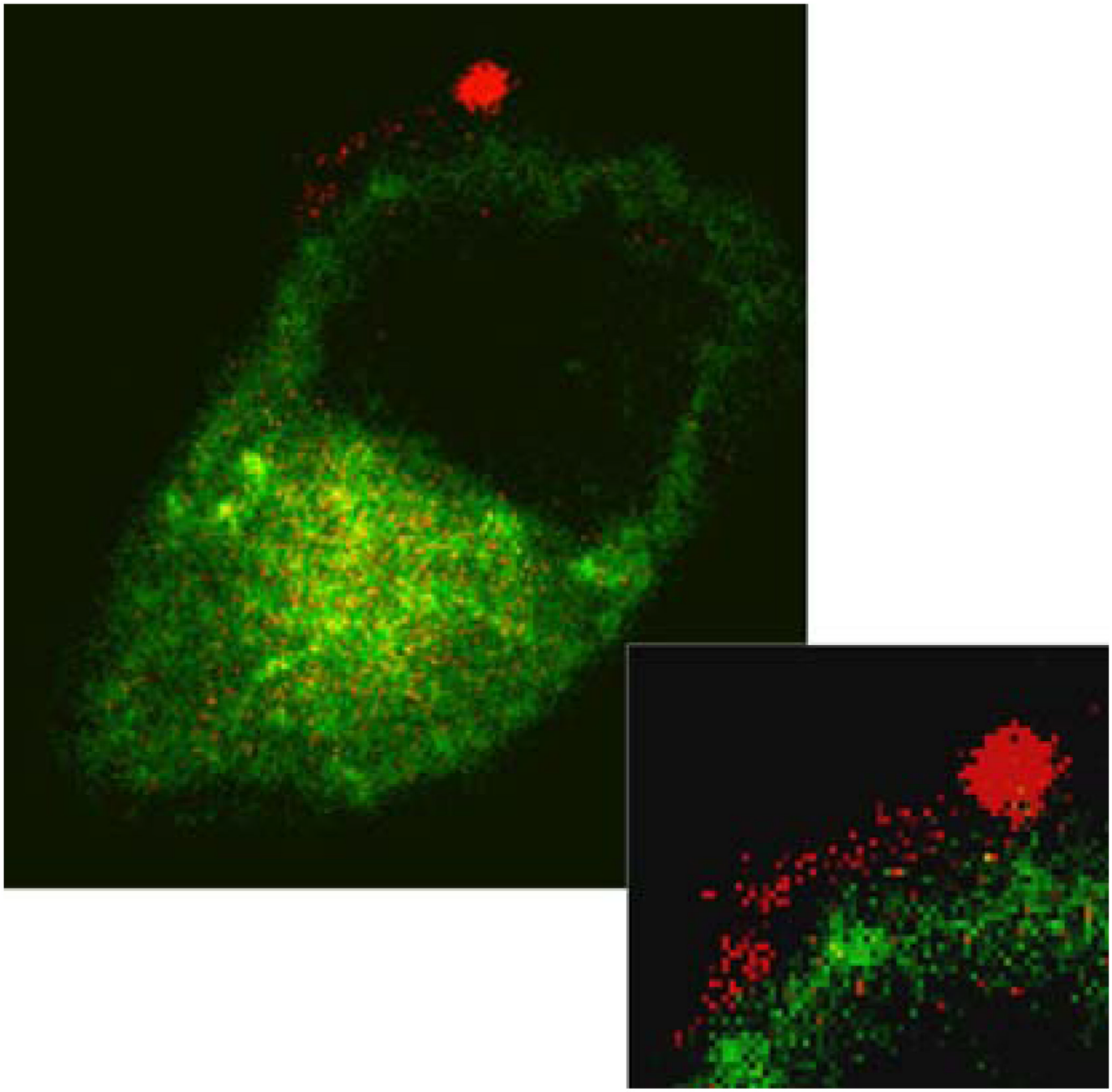

FIGURE 6.

"Lipid streaming" into the plasma membrane. A high power image of a cell surface (see inset) shows a bound rhodamine-labeled nanoparticle (red) with adjacent lipid mixing into the plasma membrane of a cell transiently expressing a green cytoplasmic marker. The cellular features that can be observed are the nucleus (dark circular region), cell cytoplasm (green), and plasma membrane (directly adjacent to cell cytoplasm, only small portion is labeled with red lipid from nanoparticle). (Reprinted with permission from Crowder *et al.*[9])

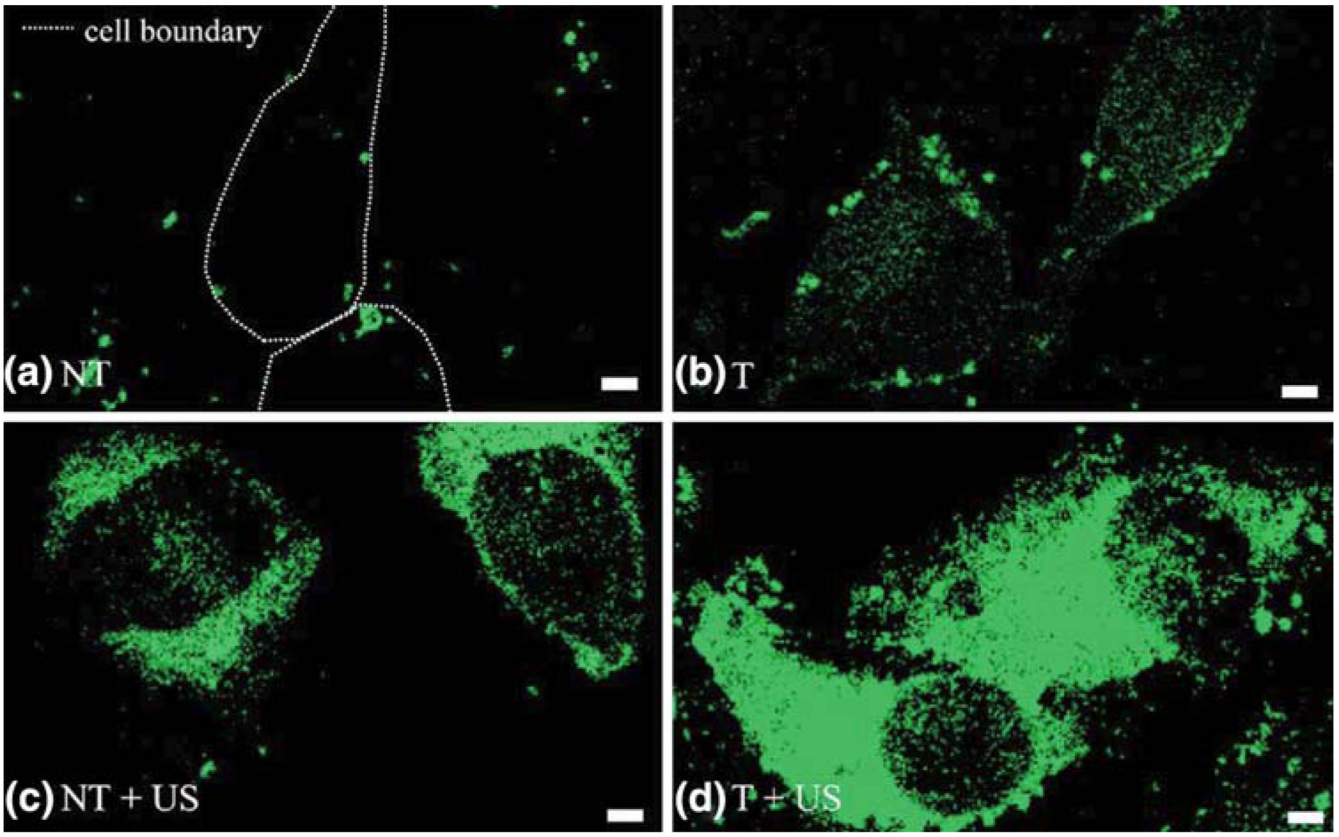

FIGURE 7.

Ultrasound energy plus targeting augment lipophilic delivery to C32 melanoma cells. Fluorescent lipid transferred from nanoparticles is green. (a) Confocal micrographs under normal conditions for nontargeted (NT) cells show minimal nonspecific internalization (dashed line indicates cell boundary). (b) $\alpha_v\beta_3$ integrin targeted (T) cells demonstrate specific targeting of nanoparticles to cell surface (green dots) and delivery of lipids in cell cytoplasm (diffuse green). (c) and (d) After ultrasound (US) insonification for 5 min, marked enhancement of cytoplasmic lipid delivery (diffuse green) was observed for both nontargeted (c) and targeted (d) cells, with the most dramatic effect for the targeted nanoparticles *with insonification* (d). The cell components observed are the nucleus (dark circular region) cell cytoplasm (bright interior), and cell membrane (bright borders). Scale bar: 2 mm. (Reprinted with permission from Crowder *et al.*[9])

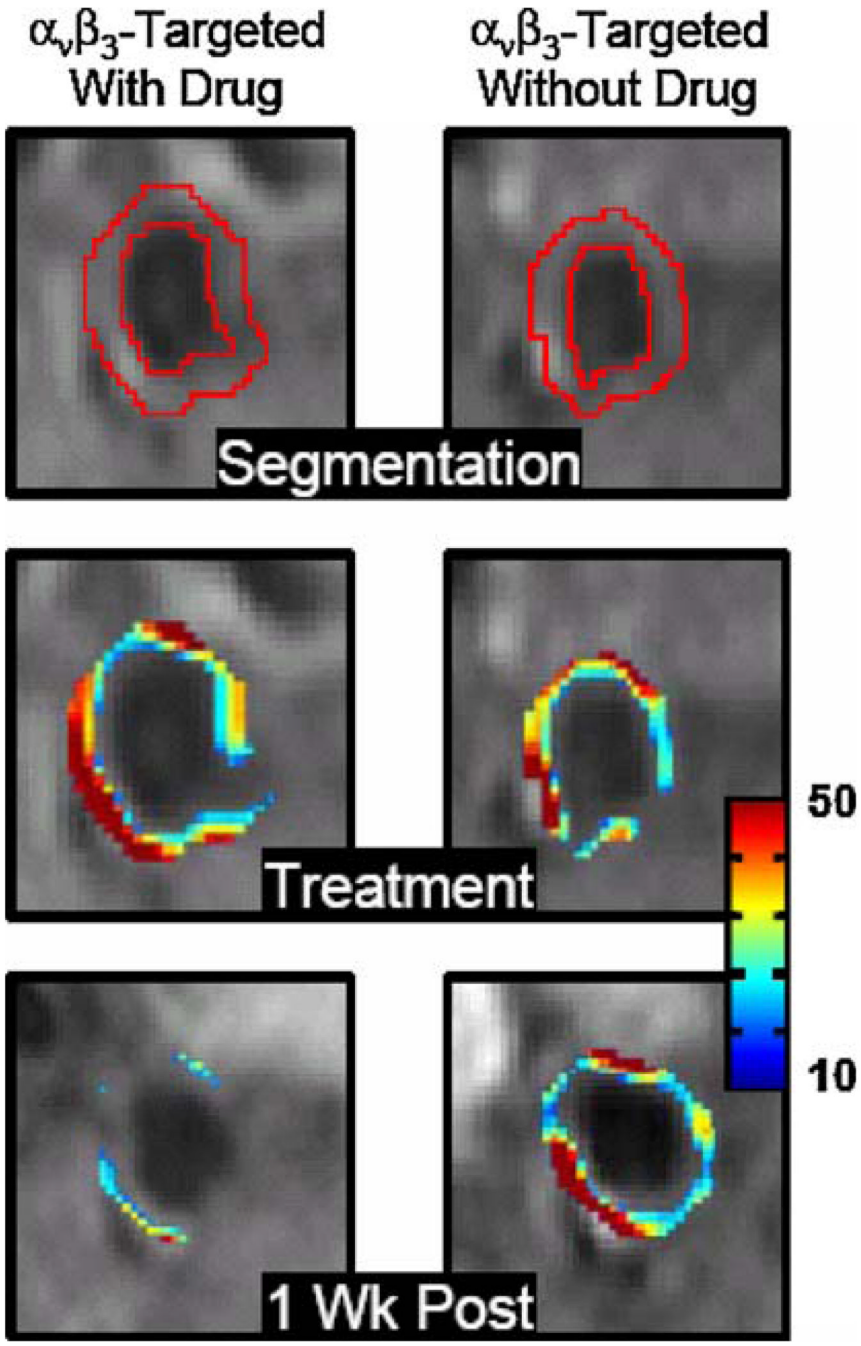

FIGURE 8.

Cross-sectional MR images of rabbit abdominal aorta showing segmented ROI (top), false-colored overlay of percent signal enhancement at time of treatment (middle) and one week post-treatment (bottom). Similar enhancement was noted at the time of treatment via $\alpha_v\beta_3$-integrin targeted paramagnetic nanoparticles either with (left) or without fumagillin (right), indicating successful delivery of nanoparticles to the vasa vasorum. One week after treatment, molecular imaging following reinjection of $\alpha_v\beta_3$-integrin targeted paramagnetic nanoparticles (no drug) revealed markedly reduced angiogenesis in animals treated with $\alpha_v\beta_3$-integrin targeted fumagillin nanoparticles vs. their no drug counterparts. (Reprinted with permission from Winter *et al.*[52])

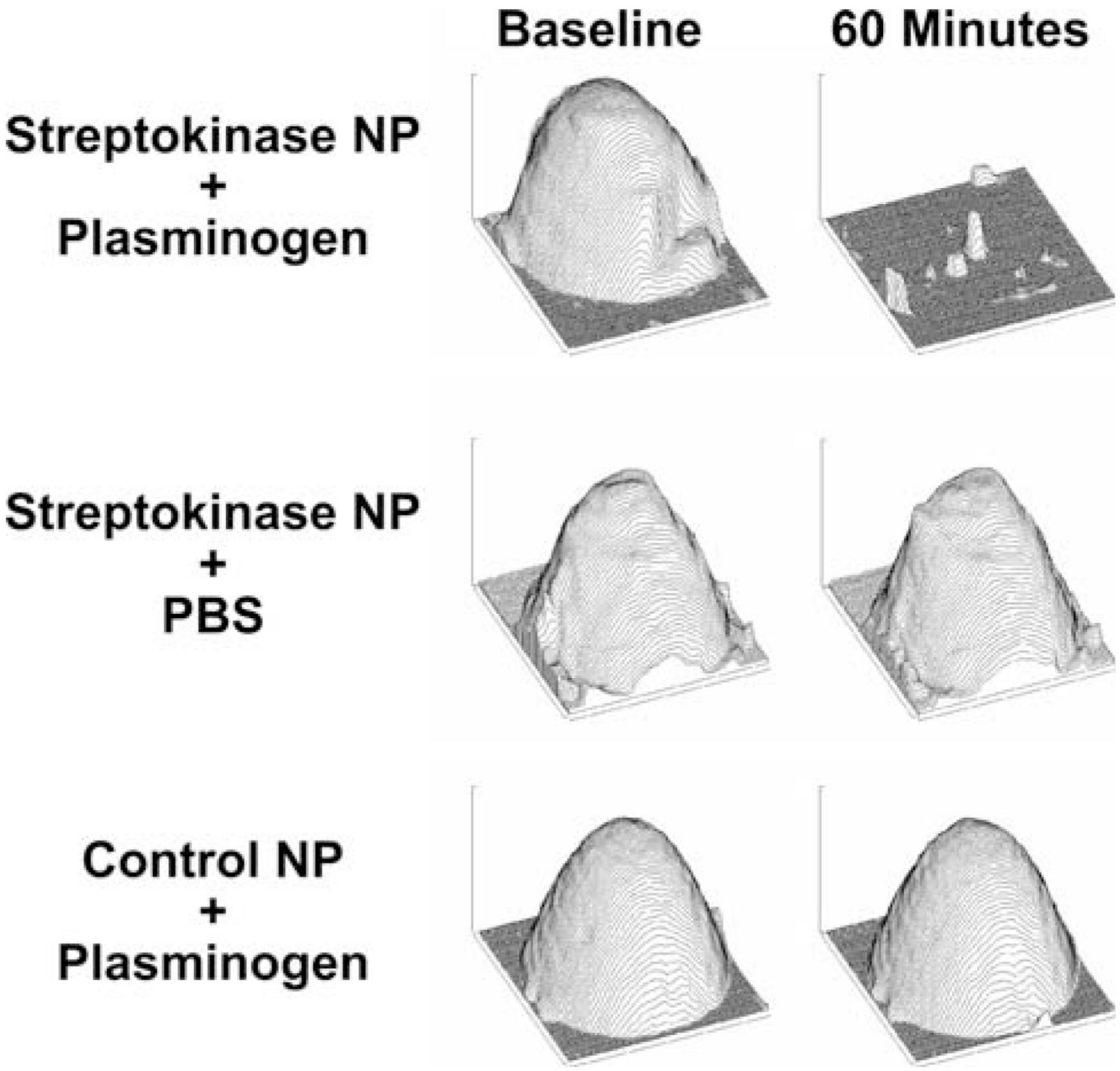

FIGURE 9.

Fibrin-targeted nanoparticle thrombolytic therapy. Experimental clot profiles detected with ultrasound after nanoparticle binding for treatment groups at baseline (left column) and after 60 min (right column). Middle and bottom rows are control groups; only the group in the top row (treated with streptokinase-modified nanoparticles in plasminogen enriched buffer) exhibits volume change with time, since streptokinase must activate plasminogen to achieve clot lytic activity. (Reprinted with permission from Marsh *et al.*[29])